



**HAL**  
open science

## **Virus-to-prokaryote ratio in spring waters along a gradient of natural radioactivity**

Lory-Anne Baker, David G Biron, Aude Beauger, Sofia Kolovi, Jonathan Colombet, Elisabeth Allain, Olivier Voltaire, Vincent Breton, Patrick Chardon, Téléphore Sime-Ngando, et al.

### ► To cite this version:

Lory-Anne Baker, David G Biron, Aude Beauger, Sofia Kolovi, Jonathan Colombet, et al.. Virus-to-prokaryote ratio in spring waters along a gradient of natural radioactivity. *Hydrobiologia*, 2023, 850 (Mars 2023), pp.1109-1121. 10.1007/s10750-023-05146-1 . hal-03979377

**HAL Id: hal-03979377**

**<https://hal.science/hal-03979377v1>**

Submitted on 8 Feb 2023

**HAL** is a multi-disciplinary open access archive for the deposit and dissemination of scientific research documents, whether they are published or not. The documents may come from teaching and research institutions in France or abroad, or from public or private research centers.

L'archive ouverte pluridisciplinaire **HAL**, est destinée au dépôt et à la diffusion de documents scientifiques de niveau recherche, publiés ou non, émanant des établissements d'enseignement et de recherche français ou étrangers, des laboratoires publics ou privés.

# Virus-to-prokaryote ratio in spring waters along a gradient of natural radioactivity

Accepted Version - Hydrobiologia

Lory-Anne Baker<sup>1,2</sup>, David G. Biron<sup>† 1,2</sup>, Aude Beauger<sup>2,3</sup>, Sofia Kolovi<sup>2,4</sup>, Jonathan Colombet<sup>1,2</sup>, Elisabeth Allain<sup>2,3</sup>, Olivier Voldoire<sup>2,3</sup>, Vincent Breton<sup>2,4</sup>, Patrick Chardon<sup>2,4</sup>, Téléphore Sime-Ngando<sup>1</sup>, Karine David<sup>2,5</sup>, Gilles Montavon<sup>2,5</sup>, Hervé Michel<sup>2,6</sup>, and Angia Sriram Pradeep Ram<sup>1\*</sup>

<sup>1</sup> Université Clermont Auvergne, CNRS, LMGE, F-63000 Clermont-Ferrand, France

<sup>2</sup> LTSER “Zone Atelier Territoires Uranifères”, F-63000 Clermont-Ferrand, 63178 Aubière Cedex, France

<sup>3</sup> Université Clermont Auvergne, CNRS, GEOLAB, F-63000 Clermont-Ferrand, France

<sup>4</sup> Université Clermont Auvergne, CNRS/IN2P3, Laboratoire de Physique de Clermont (LPC), UMR 6533, F-63178 Aubière Cedex, France

<sup>5</sup> Laboratoire SUBATECH, UMR 6457, IN2P3/CNRS/IMT Atlantique/Université de Nantes, 4, rue Alfred Kastler, BP 20722, 44307 Nantes Cedex 3, France

<sup>6</sup> Institut de Chimie de Nice (ICN), UMR 7272, Université Côte d’Azur, 28 Avenue Valrose, 06108 Nice Cedex 2, France

<sup>†</sup> deceased

## Statements and Declarations

**Conflicts of Interest:** The authors declare no conflict of interest.

## Author Contributions:

Conceptualization, Biron D.G. and Pradeep Ram A.S.; methodology, Pradeep Ram A.S., Beauger A., Allain E., Voldoire O., Colombet J., Kolovi S., Chardon P., Breton V., Karine D., Montavon G, and Michel H ; formal analysis, Baker L.-A. with the inputs from the other authors.; data curation, Baker L.-A.; writing—original draft preparation, Baker L.-A.; writing—review and editing, Baker L.-A, Pradeep Ram A.S., Sime-Ngando T with the inputs from the other authors ; supervision, Biron D.G., Pradeep Ram A.S. and Beauger A; project administration, Biron D.G. and Pradeep Ram A.S.; funding acquisition, Beauger A. and Biron D.G. All authors have read and agreed to the published version of the manuscript.

**Funding:** This study was funded by a grant from CNRS through the 80|Prime program (project acronym: DISCOVER) including a CNRS doctoral grant for L.A. BAKER. We

36 acknowledge financial support from CNRS-INEE within the context of the Zone Atelier  
37 Territoires Uranifères.

38

39 **Data availability statement:** All data generated or analysed during this study are included in  
40 this published article [and its supplementary information files].

41

42 **Acknowledgments:** We acknowledge technical support from the Zone Atelier Territoires  
43 Uranifères and from the Cytometry, Sort & Transmission Electronic Microscopy (CYSTEM)  
44 located on the campus of the University of Clermont Auvergne. We also acknowledge the  
45 three anonymous reviewers for their inputs and suggestions which greatly improved the  
46 quality of the manuscript.

47

48 **ORCID :**

49 Lory-Anne Baker <https://orcid.org/0000-0002-8346-8578>

50 David G. Biron <https://orcid.org/0000-0002-6531-4647>

51 Aude Beauger <https://orcid.org/0000-0002-0911-0500>

52 Sofia Kolovi <https://orcid.org/0000-0003-4778-2823>

53 Jonathan Colombet <https://orcid.org/0000-0003-3763-6566>

54 Elisabeth Allain <https://orcid.org/0000-0002-6411-5873>

55 Olivier Voltaire <https://orcid.org/0000-0003-1306-3054>

56 Vincent Breton <https://orcid.org/0000-0001-8197-7080>

57 Telesphore Sime-Ngando <https://orcid.org/0000-0002-7240-5803>

58 Karine David <https://orcid.org/0000-0003-0977-5905>

59 Gilles Montavon <https://orcid.org/0000-0002-3049-0106>

60 Angia Sriram Pradeep Ram <https://orcid.org/0000-0002-5469-0452>

61

62

63 Running title: Viral abundances in radioactive mineral springs

64

65

66 \*Corresponding author:

67 Angia Sriram Pradeep Ram,

68 Laboratoire Microorganismes : Génome et Environnement,

69 UMR CNRS 6023,

70 Université Clermont-Auvergne,

71 1 Impasse Amélie Murat,

72 63178, Aubière Cedex,

73 France

74 Email : [pradeep\\_ram.angia\\_sriram@uca.fr](mailto:pradeep_ram.angia_sriram@uca.fr)

75 Telephone: +33 473407463 Fax: +33 473407670

76 **Abstract** Although a strong link between viruses and prokaryotes is commonly known to  
77 exist in aquatic systems, few studies have investigated their relationship in spring waters. In  
78 the French Massif Central, certain springs are known to exhibit varying levels of naturally  
79 occurring radioactivity. Therefore, the aim of this study was to examine the standing stock of  
80 viruses together with prokaryotes, and determine the potential environmental factors  
81 influencing them in springs characterized by contrasted radioactivity gradient. Among the  
82 investigated 15 spring habitats, flow cytometry analyses indicated that both viral (VA) and  
83 prokaryotic abundances (PA) varied by an order of magnitude accompanied by virus-to-  
84 prokaryote ratio ranging between 8 and 144.2. Significant differences in VA was evident  
85 among springs where low abundances (mean  $\pm$  SD:  $21.3 \pm 7.0 \times 10^7$  VLP l<sup>-1</sup>) corresponded to  
86 high (mean  $\pm$  SD:  $1911 \pm 814.0$  nGy.h<sup>-1</sup>) gamma ( $\gamma$ ) dose radiation (<sup>222</sup>Rn) and vice versa.  
87 Adverse effect of water radioactivity (<sup>222</sup>Rn) on VA could perhaps corroborate our hypothesis  
88 of drastic effect of ionizing radiations on viruses, which might explain for lack of significant  
89 relationship between PA and VA. In such a scenario of prevailing low VA, the adopted phage  
90 life strategies could define their existence in these specialized ecosystems.

91  
92 **Keywords:** viruses; prokaryotes; virus to prokaryote ratio, mineral springs; naturally  
93 enhanced radioactivity; extreme environment.

94

95 **Introduction**

96 Viruses are found wherever life occurs, and current estimates suggest that they are the most  
97 abundant and diversified biotic agents in aquatic systems (Weinbauer, 2004; Breitbart, 2012;  
98 Schweichhart, 2021). Their omnipresence in wide variety of aquatic habitats is undoubtedly  
99 through the existence of two major pathways, namely lytic and lysogeny to confront  
100 environmental challenges (Suttle, 2007; Sime-Ngando, 2014). Viruses not only play an  
101 important role in microbial dynamics and evolution but also influence nutrients and carbon  
102 cycles through the release of dissolved organic matter during lysis which is referred to as  
103 “viral shunt” (Whitman et al., 1998). This dissolved organic matter is directly available for  
104 non-targeted prokaryotic population which stimulates their growth and activity (Wilhelm &  
105 Suttle, 1999). In aquatic systems, prokaryotes serve as principle hosts for viruses  
106 (bacteriophages) owing to their numerical dominance. As actors of cellular lysis, viruses can  
107 directly affect prokaryotic abundances as well as their structure, which probably depends on  
108 the contact rates between them (Parikka et al. 2017). Since viruses are entirely dependent on  
109 the host cells for their proliferation, a positive correlation between viruses and prokaryotes  
110 abundances can be expected. Accordingly, several studies have highlighted the existence of  
111 such a significant relationship between them in marine (Bongiorni et al., 2005; Bettarel et al.,  
112 2008), freshwater (Peduzzi & Schiemers, 2004; Brum et al., 2005) and glacier environments  
113 (Anesio et al., 2007; Rassner et al., 2016). However, some exceptional studies have reported  
114 the absence of any relationship between viruses and prokaryotes abundances (Leff et al.,  
115 1999; De Corte et al., 2010; Kyle & Ferris, 2013).

116 Although viruses are generally accepted as key players in aquatic food web, relatively little  
117 is known on the factors (abiotic and biotic) influencing them in spring habitats. A lack of  
118 opportunity to document viral ecology in such specialised systems has resulted in paucity of  
119 knowledge about these environments. Freshwater springs are small water bodies that act as  
120 crucial interfaces within the Earth’s Critical Zone. They serve as multiple three-way ecotones  
121 that link terrestrial and aquatic habitats, ground and surface waters (Reiss & Chiffard, 2017).  
122 To our knowledge virus-prokaryote interactions have been investigated in high temperature  
123 environments such as hot springs (Breitbart et al., 2004; Kepner, 2015) and deep-sea  
124 hydrothermal vent systems (Williamson et al., 2008) focussing principally on microbial  
125 compositions and dynamics. A study carried out in the terrestrial hot fluid system situated in  
126 cold environment of Southern hemisphere (French Southern and Antarctic lands) have

127 reported a significant positive relation between viruses and prokaryotes accompanied by a low  
128 virus-to-prokaryote ratio (Parikka et al., 2018).

129 The Auvergne region of the French Massif Central harbours a wide variety of mineral  
130 springs that are characterised by diverse groups of microbial communities (Lai et al., 2019,  
131 Millan et al., 2019). Due to the presence of high levels of uranium in their granitic ground,  
132 some of the mineral springs exhibit enhanced levels of natural radioactivity together with  
133 varying physico-chemical conditions. Microbes inhabiting in these environments are highly  
134 adapted and known to survive in mineralized and extreme ionizing conditions that are  
135 eventually seen as chronic stress for their survival (Shukla et al., 2017). Lethal effects of  
136 radioactivity on organisms are real due to their detrimental capability to alter their DNA  
137 structure (Ravanat & Douki, 2016). Some micro-organisms, notably prokaryotes have  
138 developed biological mechanisms to resist and tolerate high concentrations of radionuclides  
139 through DNA repair mechanisms. Genome size is also a parameter implicated in resisting  
140 high levels of radiations (Shuryak, 2019). Prokaryotes can accumulate radionuclides either in  
141 their intracellular compartment (bioaccumulation) or on their external membrane  
142 (biosorption) (Tabak et al., 2005). Henceforth, ionising radiation can induce radiobiological  
143 effects that lead to the inactivation of cells or viruses (Lea, 1946; Sullivan et al., 1971). The  
144 direct destructive effect of these radiation can produce simple or double strand breaks in  
145 nucleic acid chains (Ravanat & Douki, 2016), whereas the indirect consequence results in the  
146 production of reactive oxygen species (ROS) through water radiolysis. A correlation between  
147 the size of the virus and inactivation dose was made. The smaller the virus, higher the dose is  
148 required to inactivate it (Lea, 1946). Apart from laboratory studies, no effort has been made to  
149 determine the abundance and dynamics of naturally occurring environmental phage  
150 communities in freshwater springs. Henceforth, we hypothesize viral abundances to decrease  
151 with increasing radioactivity due to the effects of ionizing radiation, even if this radiation is of  
152 natural origin. The purpose of this study was to gain insight into (1) viral and prokaryotic  
153 abundances in a set of mineral springs along a gradient of naturally enhanced radioactivity  
154 and (2) to determine the influence of environmental factors, especially  $\gamma$ -ray radiation and  
155 activities of radionuclides belonging to the uranium decay chain, on viral and prokaryote  
156 abundances. The present study is one of the few which assess virus-prokaryote relation in  
157 mineral springs which are characterised with variable levels of naturally occurring  
158 radioactivity.

159

160 **Materials and methods**

161

### 162 ***Site description and sampling***

163 The sampling campaign was carried out in autumn from October to November 2019, where  
164 water samples were collected from a total of 15 mineral springs distributed in the Auvergne  
165 region of the French Massif Central (Fig. 1). At each site, water samples were collected in  
166 triplicates (i.e. from three independent sampling procedures). The study sites were chosen  
167 based on their physical, chemical and radiological characteristics in order to include an  
168 increasing gradient of natural radioactivity. The radioactivity comes from the decay chains of  
169 three radioelements  $^{235}\text{U}$ ,  $^{238}\text{U}$  and  $^{232}\text{Th}$  that are naturally present in the earth crust, especially  
170 in granite rocks. The disintegration of these radioelements and their daughters result in the  
171 emission of ionizing particles including  $\gamma$ -particles that can be detected at spring water  
172 surfaces. The sampling at 13 out of 15 sites was conducted in October, whereas for Montagne  
173 1 and Montagne 2 sites it was done in November (Supplementary Table 1).

174

### 175 ***Physical and chemical analyses***

176 At the 15 sampling sites, water temperature, conductivity and pH were measured with a multi-  
177 parameter WTW probe FC 340i (VWR International, Radnor, PA, USA) by submerging the  
178 probe in the spring water. Percentage saturation of dissolved oxygen was obtained with a Ysi  
179 ProODO oxygen probe (Yellow Springs Instruments, OH, USA). Bicarbonate ( $\text{HCO}_3^-$ )  
180 concentrations were determined using Hach Carbonate AL-DT kit (Hach, Loveland, CO,  
181 USA). For chemical analyses, 200 ml of water were initially filtered with Whatman GF/C  
182 filters. The filtered samples were then analyzed by high pressure ion chromatography technic,  
183 using a Thermo Scientific Dionex ICS1100 system (Thermo Fisher Scientific, Courtaboeuf,  
184 France) for cations [sodium ( $\text{Na}^+$ ), magnesium ( $\text{Mg}^{2+}$ ) and ammonium ( $\text{NH}_4^+$ )] and a Thermo  
185 Scientific Dionex Aquion system (Thermo Fisher Scientific, Courtaboeuf, France) for anions  
186 (chloride ( $\text{Cl}^-$ ) and nitrate ( $\text{NO}_3^-$ )).

187

### 188 ***Radiological characterization***

189 Gamma ( $\gamma$ -ray) dosimetry measurements were conducted just above the water surface near to  
190 the emergence of each spring using a Colibri radiometer (Mirion Technology, CA, USA), as a  
191 qualitative indicator of water radioactivity. Dose radiation (DR) measurements were  
192 performed for 2 min. and repeated for at least two times in each mineral spring to reduce the  
193 statistical uncertainties.

194 For the measurements of dissolved  $^{222}\text{Rn}$  activity in each spring, Marinelli beakers (1 L)  
195 were used to sample water from the mineral springs. A well-shaped Germanium detector  
196 (Canberra) operated at Clermont Physics Laboratory (Université Clermont Auvergne,  
197 Aubière, France) was used to measure the  $^{222}\text{Rn}$  activity. For other radiological analyses,  
198 water samples were collected in clean recipients from the water-column either near the  
199 emergence of some springs or at its outlet. Since the distance of each mineral spring to the  
200 laboratory was different, utmost care was taken to transport the water samples in refrigerated  
201 boxes to the laboratory, where they were processed immediately.

202 In addition to characterizing the ambient radiation dose and the  $^{222}\text{Rn}$  activity in water, it is  
203 also important to determine the possible contribution of radioactivity in relation to dissolved  
204 radionuclides. Among those present, we focused on the most abundant long-lived isotope  
205 ( $^{238}\text{U}$ ) as well as the descendants of this chain which are known to be highly radiotoxic (alpha  
206 particle emitters), i.e.  $^{226}\text{Ra}$  and  $^{210}\text{Po}$ . The analyses were conducted at Subatech (Nantes,  
207 France) and ICN (Nice, France) laboratories after PTFE filtration ( $0.45\mu\text{m}$ ) and acidification.  
208 Uranium was analyzed by ICP-QMS (Xseries 2, Thermo Electron). Ultra-trace concentrations  
209 of  $^{226}\text{Ra}$  were measured without chemical purification by HR-ICP-MS in low resolution mode  
210 (Element XR, Thermo Scientific) with an APEX-Q high sensitivity desolvating sample  
211 solution introduction system. In order to remove major polyatomic interferences from  $^{226}\text{Ra}$   
212 spectrum in low resolution mode, preliminary analyses were performed in medium resolution  
213 mode, where major interferences are resolved. The good consistency of  $^{226}\text{Ra}$  concentration  
214 measured in both low and medium resolution modes showed evidence of no significant  
215 production rate of major interferences (Verlinde et al., 2019). The preference to use low  
216 resolution mode for  $^{226}\text{Ra}$  was characterized by a high sensitivity ( $4.7\times 10^5$  CPS/Bq.  $\text{ml}^{-1}$ ) and  
217 a low instrumental detection limit ( $0.8$  mBq. $\text{l}^{-1}$ ). Pb and Bi-based polyatomic interferences  
218 unresolved in low and medium resolution modes were not considered in the present study due  
219 to low signal intensities measured for Pb ( $< 60,000$  CPS) and Bi ( $< 1\ 000$  CPS). Finally,  $^{210}\text{Po}$   
220 was measured, after spontaneous deposition onto a silver disc, by alpha spectrometry using  
221 dual alpha spectrometers EG&G Ortec 576A equipped with boron-implanted silicon detectors  
222 (Le et al., 2019).

223

#### 224 ***Abundances of viruses and prokaryotes***

225 For enumeration of viruses (expressed as viral like particles, VLP) and prokaryotes by flow  
226 cytometry, 2 ml of water samples were fixed with paraformaldehyde at 0.5% final  
227 concentration and transported to the laboratory in quick time ( $< 2$  hours) on ice and in the

228 dark for immediate analysis. The optimized flow cytometry protocol (different sample  
229 dilutions, threshold levels, flow rates, etc.) for the enumeration of prokaryotes and viruses  
230 from our previous investigations in French Massif Central lakes was adopted (Pradeep Ram et  
231 al. 2014). Prior to analysis, samples were diluted with 0.02  $\mu\text{m}$  filtered TE buffer (10 mM  
232 Tris-HCl and 1 mM EDTA, pH 8) and stained with nucleic acid-specific green fluorescent  
233 dye SYBR Green I (Molecular Probes, Oregon, USA) at a final concentration of  $0.5 \times 10^{-4}$   
234 (for viruses) and  $1 \times 10^{-4}$  (for prokaryotes) dilution of the commercial stock. For viral  
235 samples, staining was carried out in the dark at 80 °C for 10 min, whereas for prokaryotic  
236 samples it was done at room temperature for 15 minutes. Subsequently, the viral samples  
237 were left to cool at room temperature for 5 minutes before analysis. Counts were performed  
238 on a FACS Aria Fusion SORP cytometer (BD Sciences, San Jose, CA) equipped with an air-  
239 cooled laser providing 50 mW at 488 nm with 502 long pass, and 530/30 band pass filter set-  
240 up. Groups were identified and discriminated based on their 488 nm excited right angle light  
241 scatter (SSC) and green fluorescence (530 nm wavelength) following the protocol optimized  
242 by Brussaard et al. (2010). Flow cytometric data were analyzed using CellQuest Pro software  
243 (BD Biosciences, San Jose, CA, USA; version 4.0). Control blanks consisting of TE buffer  
244 with autoclaved 0.2 $\mu\text{m}$  filtered sample at same dilution factor as the natural samples were  
245 used before proceeding with sample analysis. Very low coincidence and background  
246 fluorescent levels were detected. Identification of viral and prokaryote population via flow  
247 cytometry in a mineral spring sample together with a control blank are shown in  
248 Supplemental Figure 1.

249

### 250 *Statistical analysis*

251 Firstly, all environmental and microbial data (averaged from replicates from each sampled  
252 site) which do not follow normal distribution were standardized using the z-score  
253 normalization [(x-mean)/standard deviation)]. This transformation allows to compare  
254 variables that initially had different units. Then, a Hierarchical clustering also called  
255 ascending hierarchical classification (AHC) based on Pearson correlation was performed to  
256 identify the groups of springs that showed environmental similarities. The groups were  
257 merged with simple link or nearest neighbor grouping. Secondly, microbial abundances (i.e.  
258 prokaryotes and viruses) were log transformed and relationships between environmental and  
259 microbial variables were tested using Pearson correlation. We ordinated the relation of  
260 microbial variables with abiotic variables through a non-metric multidimensional scaling

261 plots (NMDS) scaling using the ‘metaMDS’ function with R Package Vegan in R version 2.6-  
262 2. Euclidian distance was used to measure distribution between samples.

263 Finally, the mineral springs were classified according to their radioactivity levels to test the  
264 difference in microbial abundances between classes by using the Kruskal-Wallis test. Gamma  
265 ( $\gamma$ ) dose radiation (DR) categories were created according to the mean background DR in  
266 these sites which ranged between 70 and 250 nGy.h<sup>-1</sup>. The radioactivity classes for four  
267 radionuclides variables (i.e. <sup>222</sup>Rn, <sup>238</sup>U, <sup>210</sup>Po and <sup>226</sup>Ra) were determined from the orders of  
268 magnitude observed for these variables in the sampled springs (Supplementary Table 2).

269

## 270 **Results**

### 271 *Environmental variables*

272 The environmental characteristics of the studied spring sites are shown in supplementary  
273 material (Supplementary Table 1). The mean  $\pm$  SD conductivity of the springs was 1369  $\pm$   
274 2816  $\mu$ S.cm<sup>-1</sup> with a highest value (11,830  $\mu$ S.cm<sup>-1</sup>) recorded in the most mineralized spring  
275 (Croizat). pH did not vary among the springs (Mean  $\pm$  SD = 6.6  $\pm$  0.1). Water temperature  
276 varied between 9.9 °C and 36.4 °C (Mean  $\pm$  SD = 14.7  $\pm$  6.2 °C). Gamma radiation which  
277 presented a natural radioactivity gradient in radiation dose ranged from 120 nGy.h<sup>-1</sup> (Bard 2)  
278 to 1491 nGy.h<sup>-1</sup> (Montagne 1) with a mean value of 396  $\pm$  347 nGy.h<sup>-1</sup>. For the radionuclides  
279 activities, <sup>238</sup>U ranged from 0.003 to 0.196 Bq. l<sup>-1</sup> (Mean  $\pm$  SD = 0.03  $\pm$  0.05 Bq. l<sup>-1</sup>). <sup>222</sup>Rn  
280 activity varied between 5.6 and 3,110 Bq. l<sup>-1</sup> (Mean  $\pm$  SD = 552.6  $\pm$  897.4 Bq. l<sup>-1</sup>). <sup>226</sup>Ra had  
281 values between 0.14 and 3.2 Bq. l<sup>-1</sup> (Mean  $\pm$  SD = 1.4  $\pm$  0.9 Bq. l<sup>-1</sup>). And finally, <sup>210</sup>Po showed  
282 values ranging from 10 to 392  $\mu$ Bq. l<sup>-1</sup> (Mean  $\pm$  SD = 57.1  $\pm$  101.6  $\mu$ Bq. l<sup>-1</sup>).

### 283 *Viral and prokaryotic abundances in mineral springs with variable levels of radioactivity*

284 Both viral (VA) and prokaryotic abundances (PA) were found to vary by an order of  
285 magnitude among the mineral springs (Fig. 2, Supplementary Table 3). VA and PA ranged  
286 from 4.2 x 10<sup>7</sup> to 88.5 x 10<sup>7</sup> VLP l<sup>-1</sup> (mean  $\pm$  SD = 21.1  $\pm$  21.1 x 10<sup>7</sup> VLP l<sup>-1</sup>) and 3.12 x 10<sup>7</sup>  
287 to 20 x 10<sup>7</sup> cells l<sup>-1</sup> (mean  $\pm$  SD = 3.1  $\pm$  5.3 x 10<sup>7</sup> cells l<sup>-1</sup>), respectively. The maxima of VA  
288 and PA were observed in different springs (Supplementary Table 3). The virus to prokaryote  
289 ratio (VPR) varied between 1.8 (Salut) and 144.2 (Estreys) with a mean  $\pm$  SD of 30.5  $\pm$  37.9.  
290 Interestingly VA showed a significant negative correlation with <sup>222</sup>Rn activity (R= - 0.56,  
291 p<0.05) (Table 1). VA and PA were not correlated with the other radionuclides activities  
292 (<sup>238</sup>U, <sup>210</sup>Po, <sup>226</sup>Ra) (Table 1).

293 ***Relationship of viral and prokaryotic abundances with abiotic variables***

294 The NMDS ordination allowed the samples to be distinguished into two separate groups (Fig.  
295 3). PA and VA was clustered by abiotic variables such as conductivity, temperature, DR, pH,  
296 Na, Cl, No, HCO and  $^{222}\text{Rn}$  whereas VPR was clustered by abiotic variables such as DO, Mg,  
297  $^{210}\text{Po}$ , U,  $^{226}\text{Ra}$ . However, correlation of microbial abundances with physico-chemical  
298 parameters were less robust. VA was weakly correlated ( $p < 0.05$ ) with nitrates ( $\text{NO}_3^-$ ) (0.58,  
299  $p > 0.05$ ), DR (0.52,  $p > 0.05$ ) and  $^{222}\text{Rn}$  (0.59,  $p > 0.05$ ) (Table 1). Among the sampled mineral  
300 springs, correlation between VA and PA was non-significant ( $r = 0.12$ ,  $p > 0.05$ ) (Table 1).

301 Five clusters which were created by similarity between the samples (Pearson) (Fig. 4)  
302 was grouped into two major ones. The first cluster (containing the blue and black clusters)  
303 was associated with five samples exhibiting high doses of gamma radiation (radiation dose  $\geq$   
304  $500 \text{ nGy.h}^{-1}$ ) and  $^{222}\text{Rn}$  (activity  $> 400 \text{ Bq.l}^{-1}$ ), whereas the second (containing the green, grey  
305 and blue clusters) was predominantly associated with samples that represented lower levels of  
306 radioactivity.

307 Additionally, Kruskal-Wallis test showed significant differences ( $p < 0.001$ ) between  
308 in VA between springs with low (mean  $\pm$  SD =  $16.0 \pm 7.5 \times 10^7 \text{ VLP.l}^{-1}$ ) and medium (mean  $\pm$   
309 SD =  $41.5 \pm 27.8 \times 10^7 \text{ VLP.l}^{-1}$ ) DR (Fig. 5A). Low VA were measured in springs with high  
310 DR but no significant difference was determined by the test. Also, Kruskal-Wallis showed  
311 significant differences ( $p < 0.03$ ) in VA between springs with low (mean  $\pm$  SD =  $21.3 \pm 7.0 \times$   
312  $10^7 \text{ VLP.l}^{-1}$ ) and high (mean  $\pm$  SD =  $6.9 \pm 3.4 \times 10^7 \text{ VLP.l}^{-1}$ ) level of  $^{222}\text{Rn}$  activity (Fig. 5B).  
313 Such variations or differences were not observed for PA (Supplementary Fig. 2), and VPR.

314  
315 **Discussion**

316 The spring waters collected across the study site provided a compelling opportunity to test  
317 and evaluate the impact of natural radioactivity through the gamma radiation dose and  
318 radionuclides activities on virus-prokaryote relationship.

319 Flow cytometry enumeration of viral abundances in the mineral springs fell within the  
320 lower end of values ( $10^7$ - $10^{10} \text{ VLP.l}^{-1}$ ) as previously reported from environments like aquifers  
321 (Roudnew et al., 2013) and hypersaline lakes (Jiang et al., 2004) springs. Large variability in  
322 viral and prokaryote abundances by one and two orders of magnitude respectively could be  
323 attributed to the prevailing conditions in different springs. Differences and variability in  
324 conductivity and temperature are mainly related to the depth at which groundwater has  
325 infiltrated and then, to its speed to reach the surface (Boineau & Maisonneuve, 1972). In fact,

326 the adaptability and flexibility of viruses to survive in the most mineralized spring (Croizat)  
327 with a conductivity of  $11,830 \mu\text{S}\cdot\text{cm}^{-1}$  suggest that phages are an important component of  
328 crenic communities. Studies investigating freshwater viromes have attributed to large  
329 differences in viral diversity to salinity (Tseng et al. 2013) and conductivity gradients (Roux  
330 et al. 2012). Significant relationship of nitrate to viruses rather than to prokaryotes in our  
331 study were similar to a report from a freshwater reservoir (Peduzzi and Schiemer, 2004), but  
332 however the role of nitrate in influencing viral abundance is unclear and less discussed in  
333 literature.

334 Viruses are host specific and largely rely on the availability of susceptible host cells  
335 (mainly prokaryotes) for their proliferation. However, in contrast to reports from other  
336 freshwaters systems (Peduzzi and Schiemer 2004, Pradeep Ram et al. 2014), viral and  
337 prokaryote abundances obtained in our study were not significantly correlated. Since mineral  
338 springs are restrictive and oligotrophic environments (Reiss and Chiffard 2017), it is likely  
339 that the nature and dynamics of viral strategy could influence viral and prokaryote counts in  
340 such harsh or stressful conditions. The fact that prokaryotes serve as dominant host for viruses  
341 always remains a difficult hypothesis to test. The application of recent molecular tools would  
342 help to identify specific host–virus relationships and assess their interactions.

343 Virus-to-prokaryote ratio (VPR) has often been a descriptor of relationship between  
344 viruses and prokaryotes in a given environment (Parikka et al. 2017). VPR is the result of a  
345 comprehensive balance of factors, such as viral production, transport of viruses through  
346 sinking particles, decay rates and life strategies (Wigington et al., 2016). Large variation of  
347 VPR by two orders of magnitude among the springs (1.4 to 144) is much higher than reports  
348 from hot springs located in Southern Hemisphere (0.1 to 6.0, Parikka et al. 2018), but similar  
349 to the reported range in near surface oceans (1.4 to 160, Wigington et al. 2016). The broad  
350 distribution of VPR together with a lack of significant relationship between VA and PA in the  
351 springs imply that the increase in the former is a poor qualitative predictor of latter. The  
352 observed increase in PA along with VPR has been attributed to direct dependence of viral  
353 production on PA, thus imposing additionally a possible selective pressure that can lead to a  
354 reduced volume of host cells (Hara et al. 1996). Low VPR observed in some springs could  
355 either be as a result of host cell resistance or specific phage adsorption to host when their  
356 diversity is low (Maranger et al. 1994, Tuomi et al. 1995). In our study, none of the abiotic  
357 factors were found to explain for the variation in VPR which was probably due to the  
358 differences in the prevailing environmental parameters among the study habitats. It is more  
359 likely that the factor(s) influencing VPR could be specific to each spring.

360 In the mineral springs,  $^{222}\text{Rn}$  accounted for the highest nuclear activity (number of  
361 disintegrations per time unit) compared to others radionuclides. Adverse effect of water  
362 radioactivity on viral abundance, as seen by a significant negative correlation between VA  
363 and  $^{222}\text{Rn}$  activity could perhaps corroborate our hypothesis on the drastic effect of ionizing  
364 radiation on viruses. However, the correlation between VA and the other radionuclides  
365 activities ( $^{238}\text{U}$ ,  $^{226}\text{Ra}$  and  $^{210}\text{Po}$ ) was not evident. VA varied between springs with low and  
366 medium DR. The low mean value of VA in springs with high  $^{222}\text{Rn}$  activity suggests that viral  
367 decay could be more important in these habitats.

368 Ionizing radiation or exposure to alpha particles from radon is known to generate and  
369 induce DNA mutations, chromosomes aberrations and other cellular abnormalities such as  
370 protein modification (Robertson et al., 2013; Reisz et al., 2014). Also, viral inactivation has  
371 been reported in the context of intense  $\gamma$ -ray irradiation (Sullivan et al., 1971). Irradiation of  
372 lambda phage induces DNA strand breakage and lead to the inactivation of phages (Bertram,  
373 1988). The findings from laboratory investigations could perhaps extend support to aquatic  
374 microbes, where the presence of high levels of radon might affect viral capsid integrity and  
375 prokaryotes membranes. However, phages too can appear to be more resistant to ionising  
376 radiations (Lea, 1946). In the case of prokaryotes, their membrane that enables nutrient  
377 exchange between the cell and the environment can absorb radionuclides and be subjected to  
378 external and internal irradiation. Although it has been previously hypothesized that micro-  
379 organisms are known to have colonised the spring ecosystems billions of years ago (Djokic et  
380 al. 2017), radioactivity arising from natural origin could be a stressor for them and affect the  
381 relationship between these two protagonists. In such a scenario it could be interesting to  
382 identify the adaptive strategy of viruses (lytic, lysogeny or pseudolysogeny) under  
383 challenging environmental conditions. Therefore, investigations pertaining to viral infection  
384 in mineral springs can provide important information on virus-prokaryote interaction and their  
385 mediated biogeochemical processes.

386 In conclusion, no significant correlation was found between viruses and prokaryotes in  
387 the analyzed spring waters. Among different parameters considered for natural radioactivity  
388 (radon activity, radiation dose, dissolved radionuclide activity), radon activity appears to be  
389 the most influential parameter. Low viral abundances in springs amidst of high levels of  $^{222}\text{Rn}$   
390 activity and vice versa are suggestive of drastic effect of ionizing radiation on viruses which  
391 could possibly be linked to viral decay due to DNA damage.

392

393 **References**

- 394 Anesio, A. M., B. Mindl, J. Laybourn- Parry, A. J. Hodson & B. Sattler, 2007. Viral  
395 dynamics in cryoconite holes on a high Arctic glacier (Svalbard). *Journal of*  
396 *Geophysical Research: Biogeosciences* G4. <https://doi.org/10.1029/2006JG000350>
- 397 Bettarel, Y., R. Aarfffi, T. Bouvier, M. Bouvy, E. Briand, J. Colombet, D. Corbin & T. Sime-  
398 Ngando, 2008. Virioplankton distribution and activity in a tropical eutrophicated bay.  
399 *Estuarine, Coastal and Shelf Science* 80: 425-429.  
400 <http://dx.doi.org/10.1016/j.ecss.2008.08.018>
- 401 Bertram, H, 1988. DNA damage and mutagenesis of lambda phage induced by gamma-rays.  
402 *Mutagenesis* 3: 29–33. <https://doi.org/10.1093/mutage/3.1.29>
- 403 Boineau, R. & J. Maisonneuve, 1972. Les sources minérales du Massif central français et leur  
404 cadre géologique. [The mineral springs of the French Massif central and their  
405 geological setting.] Rapport BRGM 72-SGN-151-MCE.
- 406 Bongiorno L., M. Magagnini, M. Armeni, R. Noble & R. Danovaro, 2005. Viral production,  
407 decay rates, and life strategies along a trophic gradient in the North Adriatic Sea.  
408 *Applied and Environmental Microbiology* 71: 6644-6650.  
409 <https://doi.org/10.1128/AEM.71.11.6644-6650.2005>
- 410 Breitbart, M., L. Wegley, S. Leeds, T. Schoenfeld & F. Rohwer, 2004. Phage Community  
411 Dynamics in Hot Springs. *Applied and Environmental Microbiology* 70: 1633–1640.  
412 <https://doi.org/10.1128/AEM.70.3.1633-1640.2004>
- 413 Breitbart, M. 2012. Marine viruses: Truth or dare. *Annual Review of Marine Science* 4: 425-  
414 428. <https://doi.org/10.1146/annurev-marine-120709-142805>
- 415 Brum, J. R., G. F. Steward, S. C. Jiang & R. Jellison, 2005. Spatial and temporal variability of  
416 prokaryotes, viruses, and viral infections of prokaryotes in an alkaline, hypersaline  
417 lake. *Aquatic Microbial Ecology* 41: 247-260. <http://dx.doi.org/10.3354/ame041247>
- 418 Brussaard C., J. P. Payet & M. G. Weinbauer, 2010. Quantification of aquatic viruses by flow  
419 cytometry. *Manual of Aquatic Viral Ecology* 11: 102-109.  
420 <https://dx.doi.org/10.17504/protocols.io.dpj5km>
- 421 De Corte, D., E. Sintès, C. Winter, T. Yokokawa, T. Reinthaler & G. J. Herndl, 2010. Links  
422 between viral and prokaryotic communities throughout the water column in the  
423 (sub)tropical Atlantic Ocean. *The ISME Journal* 4: 1431–1442.  
424 <https://doi.org/10.1038/ismej.2010.65>

- 425 Djokic T, Van Kranendonk MJ, Campbell KA, Walter MR, & Ward CR, 2017. Earliest signs  
426 of life on land preserved in ca. 3.5 Ga hot spring deposits. *Nature Communications* 8:  
427 15263. <https://doi.org/10.1038/ncomms15263>
- 428 Hara, S. K., Koike, K., Terauchi, H., Kamiya, H. & Tanoue, E. (1996). Abundance of viruses  
429 in deep oceanic waters. *Marine Ecological Progress Series* 145, 269–277. Jiang, S., G.  
430 Steward, R. Jellison, W. Chu & S. Choi, 2004. Abundance, distribution, and diversity  
431 of viruses in alkaline, hypersaline Mono Lake, California. *Microbial Ecology* 47: 9–  
432 17. <https://doi.org/10.1007/s00248-003-1023-x>
- 433 Kepner, R., 2015. Influence of Hot Spring Phages on Community Carbon Metabolism: Win,  
434 Lose or Draw? *Advances in Microbiology* 05: 630–43.  
435 <https://doi.org/10.4236/aim.2015.59066>
- 436 Kyle J. E. & F. G. Ferris, 2013. Geochemistry of Virus-Prokaryote Interactions in Freshwater  
437 and Acid Mine Drainage Environments, Ontario, Canada. *Geomicrobiology Journal*  
438 30: 769–778. <https://doi.org/10.1080/01490451.2013.770978>
- 439 Lai, G. G., A. Beauger, C. E. Wetzel, B. M. Padedda, O. Voldoire, A. Lugliè, E. Allain & L.  
440 Ector, 2019. Diversity, ecology and distribution of benthic diatoms in thermo-mineral  
441 springs in Auvergne (France) and Sardinia (Italy). *PeerJ*. 7: e7238.  
442 <https://doi.org/10.7717/peerj.7238>
- 443 Le, T. H. H., H. Michel & J. Champion, 2019. 210 Po sequential extraction applied to wetland  
444 soils at uranium mining sites. *Journal of Environmental Radioactivity* 199: 1-6.  
445 <https://doi.org/10.1016/j.jenvrad.2018.12.027>
- 446 Lea, D. E., 1946. The inactivation of viruses by radiations. *The British Journal of Radiology*  
447 19: 205-212. <https://doi.org/10.1259/0007-1285-19-221-205>
- 448 Leff, A. A., L. G. Leff, M. J., Lemke, R. T., Heath & X. Gao, 1999. Abundance of planktonic  
449 virus-like particles in Lake Erie subsurface waters. *The Ohio Journal of Science* 99,  
450 16–18.
- 451 Maranger, R., Bird, D. F. & Juniper, S. K. (1994). Viral and bacterial dynamics in Arctic sea  
452 ice during the spring algal bloom near Resolute, N.W.T., Canada. *Marine Ecology*  
453 *Progress Series* 111, 121–127. <http://dx.doi.org/10.3354/meps111121>
- 454 Millan, F., C., Izere, V., Breton, O., Voldoire, D. G., Biron, C. E., Wetze, D., Miallier, E.,  
455 Allain, L., Ector & A. Beauger, 2019. The effect of natural radioactivity on diatom  
456 communities in mineral springs. *Botany Letters* 8107: 95-113.  
457 <https://doi.org/10.1080/23818107.2019.1691051>

458 Peduzzi, P. & F. Schiemers, 2004. Bacteria and viruses in the water column of tropical  
459 freshwater reservoirs. *Environmental Microbiology* 6: 707-715.  
460 <https://doi.org/10.1111/j.1462-2920.2004.00602.x>

461 Parikka, K. J., M., Le Romancer, N., Wauters & S. Jacquet, 2017. Deciphering the virus-to-  
462 prokaryote ratio (VPR): Insights into virus–host relationships in a variety of  
463 ecosystems. *Biological Reviews* 92: 1081–1100. <https://doi.org/10.1111/brv.12271>

464 Parikka, K. J., S., Jacquet, J., Colombet, D., Guillaume & M. Le Romancer, 2018. Abundance  
465 and observations of thermophilic microbial and viral communities in submarine and  
466 terrestrial hot fluid systems of the French Southern and Antarctic Lands. *Polar Biology*  
467 41: 1335–1352. <https://doi.org/10.1007/s00300-018-2288-3>

468 Pradeep Ram AS, Palesse S, Colombet J, Thouvenot T & Sime-Ngando T. 2014. The relative  
469 importance of viral lysis and nanoflagellate grazing for prokaryotic mortality in  
470 temperate lakes. *Freshwater Biology*, 59: 300–11. <https://doi.org/10.1111/fwb.12265>

471 Rassner SME, Anesio AM, Girdwood SE, Hell K, Gokul JK, Whitworth DE, Edwards A,  
472 2016. Can the bacterial community of a high arctic glacier surface escape viral  
473 control? *Frontiers in Microbiology* 7: 956.  
474 <https://doi.org/10.3389/fmicb.2016.00956>

475 Ravanat, J. L. & T. Douki, 2016. UV and ionizing radiations induced DNA damage,  
476 differences and similarities. *Radiation Physics and Chemistry* 128: 92-102.  
477 <https://dx.doi.org/10.1016/j.radphyschem.2016.07.007>

478 Reiss, M. & P. Chiffard, 2017. An opinion on spring habitats within the earth’s critical zone  
479 in headwater regions. *Water* 9: 645. <https://doi.org/10.3390/w9090645>

480 Reisz, J. A., N., Bansal, J., Qian, W., Zhao & C. M. Furdui, 2014. Effects of Ionizing  
481 Radiation on Biological Molecules-Mechanisms of Damage and Emerging Methods of  
482 Detection. *Antioxidants and Redox Signaling* 21: 260–292.  
483 <https://dx.doi.org/10.1089/fars.2013.5489>

484 Robertson, A., J. Allen, R. Laney & A. Curnow, 2013. The Cellular and Molecular  
485 Carcinogenic Effects of Radon Exposure: A Review. *International Journal of*  
486 *Molecular Sciences* 14: 14024-14063. <https://dx.doi.org/10.3390/fijms140714024>

487 Roudnew, B., T. J. Lavery, J. R. Seymour, R. J. Smith & J. G. Mitchell, 2013. Spatially  
488 varying complexity of bacteria and virus-like particle communities within an aquifer  
489 system. *Aquatic Microbial Ecology* 68: 259– 266. <http://dx.doi.org/10.3354/ame01615>

490 Roux, S., Enault F, Robin A, Ravet V, Personnic S, Theil, S, Colombet J, Sime-Ngando T &  
491 Debros D. 2012. Assessing the diversity and specificity of two freshwater viral

492 communities through metagenomics. PLoS One. 7:e33641.  
493 <https://doi.org/10.1371/journal.pone.0033641>

494 Schweichhart, J. 2021. Prokaryotic viruses: Intriguing players in the aquatic stream. In  
495 Reference Module in Earth Systems and Environmental Sciences; Elsevier: Oxford,  
496 UK. <https://doi.org/10.1016/B978-0-12-819166-8.00106-7>.

497 Shukla, A., P. Parmar & M. Saraf, 2017. Radiation, radionuclides and bacteria: An in-  
498 perspective review. Journal of Environmental Radioactivity 180: 27-35.  
499 <https://doi.org/10.1016/j.jenvrad.2017.09.013>

500 Shuryak, I., 2019. Review of microbial resistance to chronic ionizing radiation exposure  
501 under environmental conditions. Journal of environmental radioactivity, 196, 50-63.  
502 <https://doi.org/10.1016/j.jenvrad.2018.10.012>

503 Sime-Ngando, T. & J. Colombet, 2009. Virus and prophages in aquatic ecosystems. Canadian  
504 Journal of Microbiology 55: 95–109. <https://doi.org/10.1139/w08-099>

505 Sime-Ngando, T., 2014. Environmental bacteriophages: Viruses of microbes in aquatic  
506 ecosystems. Frontiers in Microbiology 5: 1–14.  
507 <https://doi.org/10.3389/fmicb.2014.00355>

508 Sullivan, R., A. C. Fassolitis, E. P. Larkin, R. B. Read, J. T. Peeler & S. E. T. Al, 1971.  
509 Inactivation of Thirty Viruses by Gamma Radiation. Applied Microbiology 22: 61–65.

510 Suttle, C. A., 2007. Marine viruses - Major players in the global ecosystem. Nature Reviews  
511 Microbiology 5: 801–812. <https://doi.org/10.1038/nrmicro17503>

512 Tabak, H., P. Lens, E.D. Van Hullebusch & W. Dejonghe, 2005. Developments in  
513 bioremediation of soils and sediments polluted with metals and radionuclides–1.  
514 Microbial processes and mechanisms affecting bioremediation of metal contamination  
515 and influencing metal toxicity and transport. Environmental Science and Bio-  
516 Technology. 4: 115-156. <http://dx.doi.org/10.1007/s11157-005-2169-4>

517 Tseng, C.-H., P.-W. Chiang, F.-K. Shiah, Y.-L. Chen, J.-R. Liou, T.-C. Hsu, S.  
518 Maheswararajah, I. Saeed, S. Halgamuge, et S.-L. Tang. 2013. Microbial and viral  
519 metagenomes of a subtropical freshwater reservoir subject to climatic disturbances.  
520 ISME J. 7:2374–2386. <https://doi.org/10.1038/ismej.2013.118>

521 Tuomi, P., Fagerbakke, K. M., Bratbak, G. & Heldal, M. (1995). Nutritional enrichment of a  
522 microbial community: the effects on activity, elemental composition, community  
523 structure and virus production. FEMS Microbiology Ecology 16, 123–134.  
524 [https://doi.org/10.1016/0168-6496\(94\)00076-9](https://doi.org/10.1016/0168-6496(94)00076-9)

525 Verlinde, M., J. Gorny, G. Montavon, S. Khalfallah, B. Boulet, C. Augeray, D. Larivière, C.  
526 Dalencourt & A. Gourgiotis, 2019. A new rapid protocol for <sup>226</sup>Ra separation and  
527 preconcentration in natural water samples using molecular recognition technology for  
528 ICP-MS analysis. *Journal of Environmental Radioactivity* 202: 1-7.  
529 <https://doi.org/10.1016/j.jenvrad.2019.02.003>

530 Weinbauer, M. G. 2004, Ecology of prokaryotic viruses. *FEMS Microbiology Reviews* 28,  
531 127–81. <https://doi.org/10.1016/j.femsre.2003.08.001>

532 Whitman, W. B., D. C. Coleman & W. J. Wiebe, 1998. Prokaryotes: The unseen majority.  
533 *Proceedings of the National Academy of Sciences* 95: 6578–6583.  
534 <https://doi.org/10.1073/pnas.95.12.6578>

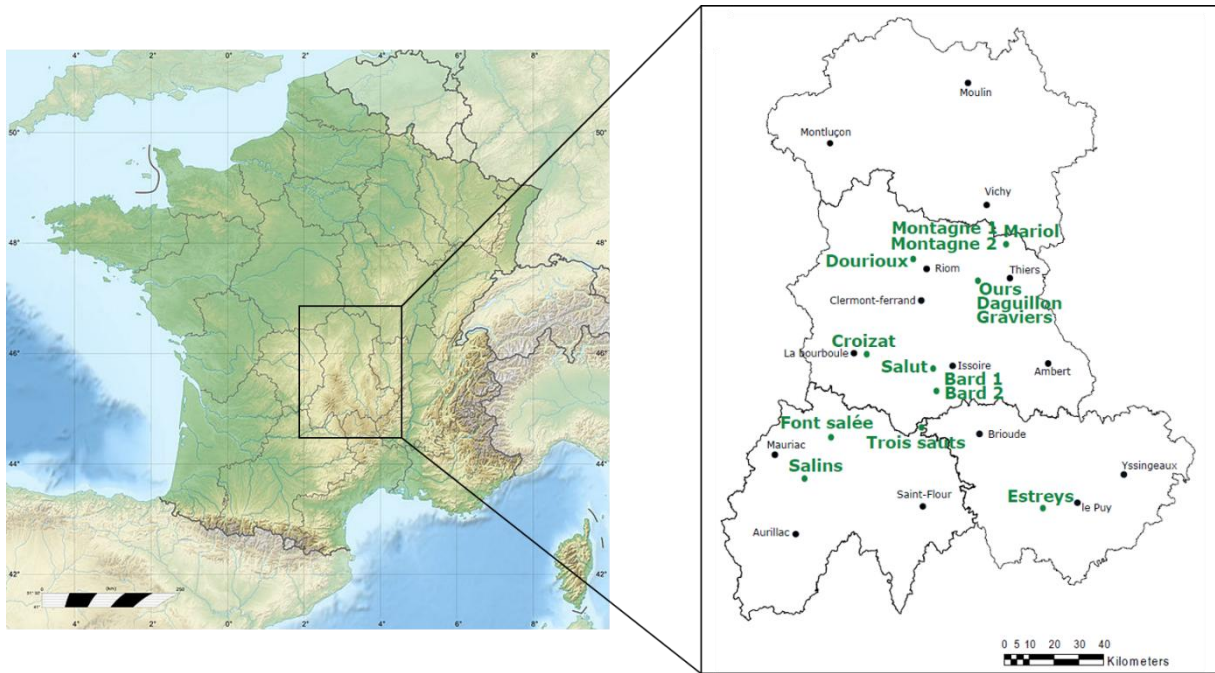
535 Wigington, C. H., D. Sonderegger, C. P. D. Brussaard, A. Buchan, J. F. Finke, J. A. Fuhrman,  
536 J. T. Lennon, M. Middelboe, C. A. Suttle, C. Stock, W. H. Wilson, K. E. Wommack,  
537 S. W. Wilhelm & J. S. Weitz, 2016. Re-examination of the relationship between  
538 marine virus and microbial cell abundances. *Nature Microbiology* 1:4–11.  
539 <https://doi.org/10.1038/nmicrobiol.2015.24>

540 Wilhelm, S. W. & A. C. Suttle, 1999. Viruses and nutrient cycles in the sea: viruses play  
541 critical roles in the structure and function of aquatic food webs. *Bioscience* 49: 781-  
542 788. <https://doi.org/10.2307/1313569>

543 Williamson, S. J., S. C. Cary, K. E. Williamson, R. R. Helton, S. R. Bench, & D. Winget,  
544 2008. Lysogenic virus-host interactions predominate at deep-sea diffuse-flow  
545 hydrothermal vents. *The ISME Journal* 2: 1112–1121.  
546 <https://doi.org/10.1038/ismej.2008.73>

547  
548  
549

550 **Fig. 1** Map showing the location of 15 mineral springs (green) in the Auvergne region of  
551 French Massif Central

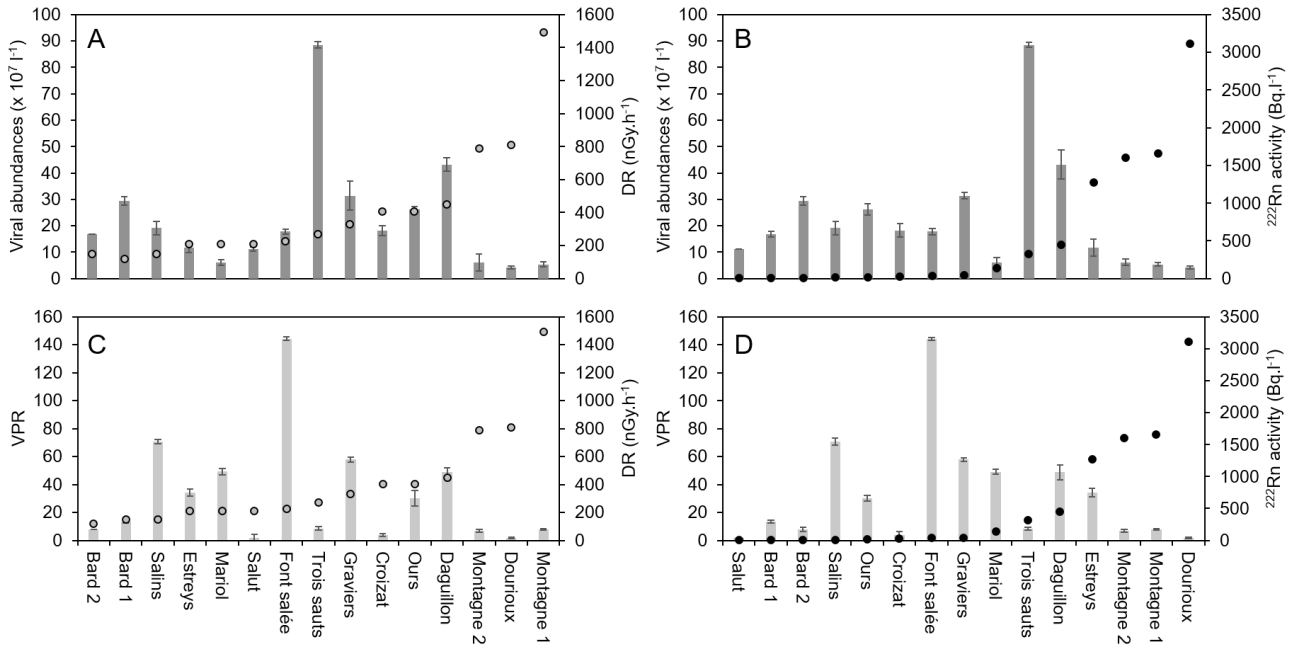


552

553

554

555 **Fig. 2** Histograms showing viral abundances (A) together with dosage radiation, DR and  
 556 (B)  $^{222}\text{Rn}$  activity and, VPR (virus to prokaryote ratio) with (C) dosage radiation, DR and  
 557 (D)  $^{222}\text{Rn}$  activity for each spring. On each histogram, the mineral springs are classified with  
 558 an increasing radioactivity gradient (DR and  $^{222}\text{Rn}$  represented in grey and black circles  
 559 respectively). Data represent mean  $\pm$  SD ( $n = 3$ ) for each sampled spring.



560

561

562

563

564

565

566

567

568

**Figure 3:** Non-metric multidimensional scaling (NMDS, stress value = 1) illustrating similarity between samples. Relations between biotic and abiotic variables are represented. HCO:  $\text{HCO}_3^-$ ; Na:  $\text{Na}^+$ ; Cl:  $\text{Cl}^-$ ; Mg:  $\text{Mg}^{2+}$ ; NO:  $\text{NO}_3^-$ ; NH:  $\text{NH}_4$ ; Cond: conductivity; Temp: temperature; DO: dissolved oxygen;  $\text{U}^{238}$ : U activity; Ra:  $^{226}\text{Ra}$ ; Rn:  $^{222}\text{Rn}$ ; Po:  $^{210}\text{Po}$ ; DR: dose radiation; VA: viral abundance, PA: prokaryote abundance; VPR: viral-prokaryote ratio.

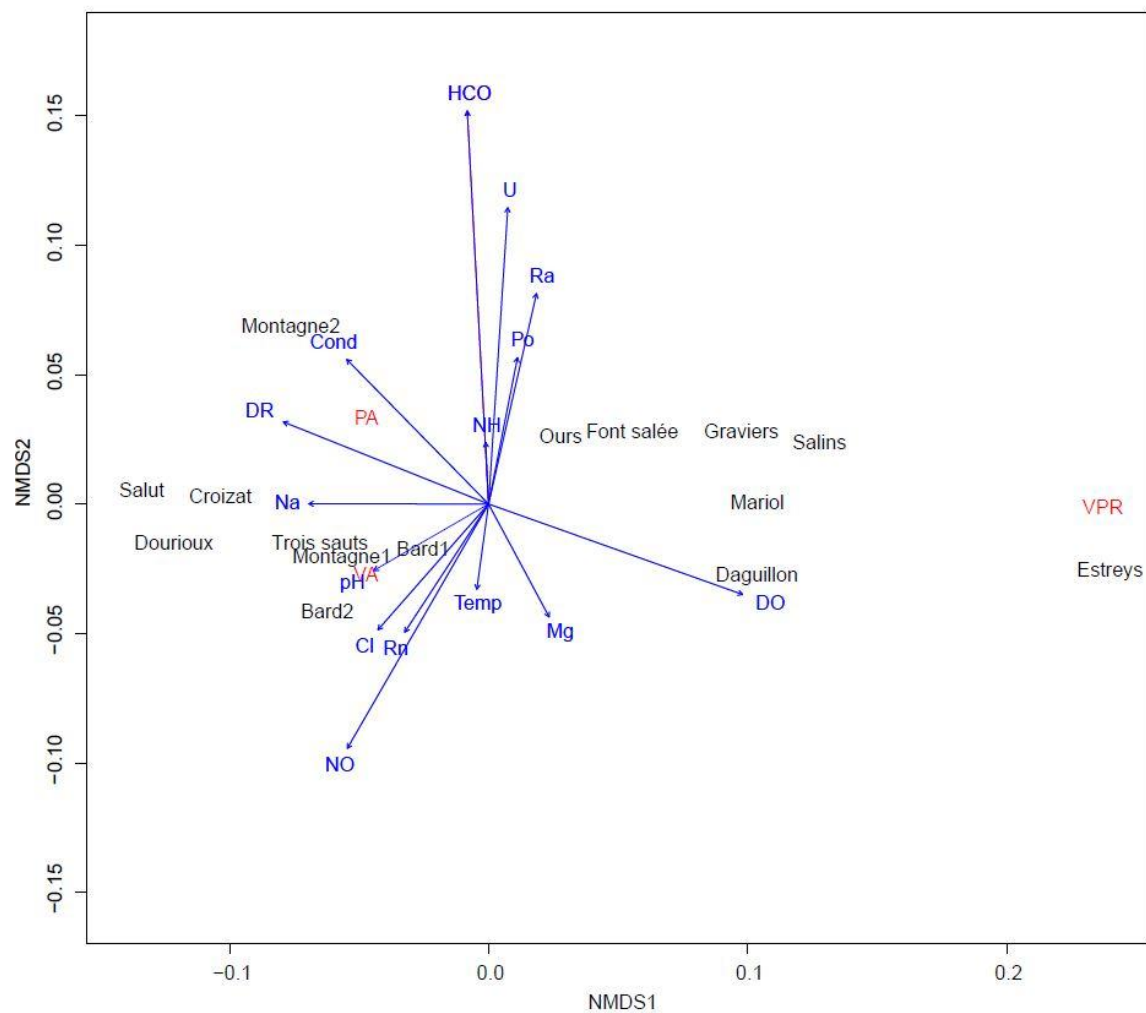
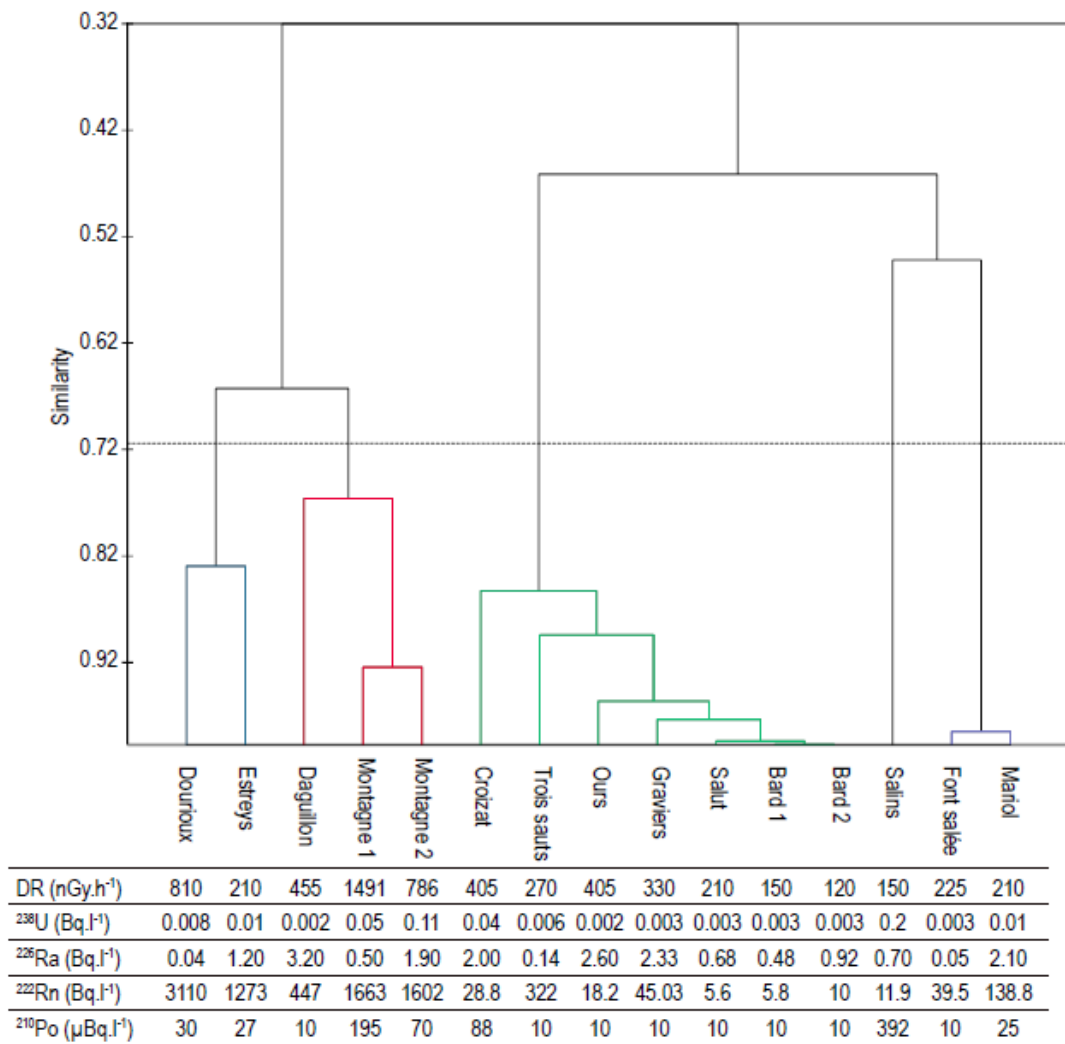


**Fig. 4** Dendrogram based on hierarchical ascendant classification analysis (HAC) of springs performed on physical, chemical and radioactive parameters measured. DR: dose radiation,  $^{222}\text{Rn}$ :  $^{222}\text{Rn}$  activity,  $^{238}\text{U}$ :  $^{238}\text{U}$  activity,  $^{210}\text{Po}$ :  $^{210}\text{Po}$  activity,  $^{226}\text{Ra}$ :  $^{226}\text{Ra}$  activity.



**Values of radioactive parameters measured in each springs**

**Figure 5:** Kruskal-Wallis tests on differences in the mean viral abundances in mineral springs classified by (A) gamma ( $\gamma$ ) dose radiation (DR) (3 classes: Low:  $DR < 250 \text{ nGy.h}^{-1}$  (7 sites); Medium:  $250 \text{ nGy.h}^{-1} \geq DR \leq 500 \text{ nGy.h}^{-1}$  (5 sites); High:  $DR > 500 \text{ nGy.h}^{-1}$  (3 sites) and (B)  $^{222}\text{Rn}$  activity levels (3 classes: Low: activity  $< 100 \text{ Bq.l}^{-1}$  (8 sites); Medium:  $100 \text{ Bq.l}^{-1} \geq \text{activity} \leq 1000 \text{ Bq.l}^{-1}$  (3 sites); High: activity  $> 1000 \text{ Bq.l}^{-1}$  (4 sites). Red crosses represent the mean value with SD calculated for each level based on the number of sites. Star indicates significant p value ( $p < 0.05$ ).

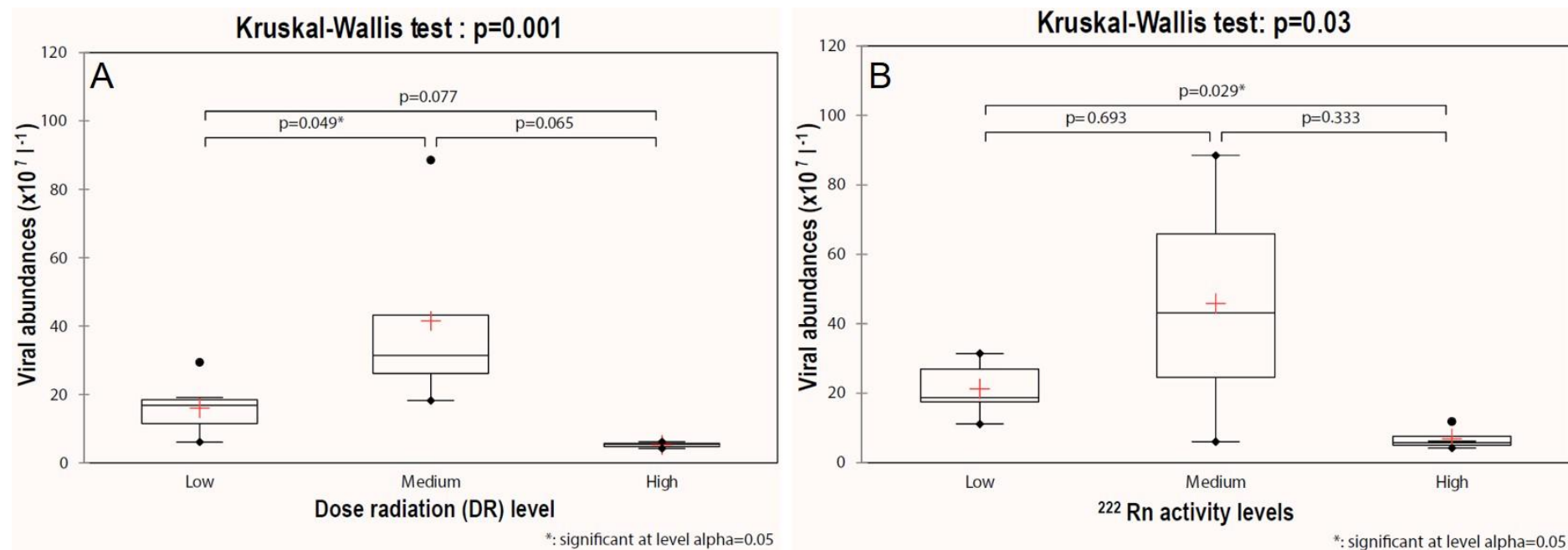


**Table 1** Pearson correlation coefficient (r) between microbial and abiotic parameters (n=15).

	VA	PA	VPR	pH	DO	Temp	Cond	Na <sup>+</sup>	Mg <sup>2+</sup>	Cl <sup>-</sup>	NO <sub>3</sub> <sup>-</sup>	NH <sub>4</sub> <sup>+</sup>	HCO <sub>3</sub> <sup>-</sup>	<sup>238</sup> U	<sup>226</sup> Ra	<sup>222</sup> Rn	<sup>210</sup> Po
VA	<b>1.00</b>	0.12	0.17	0.39	0.51	0.17	-0.02	0.08	0.46	0.20	<b>-0.58</b>	0.38	-0.40	-0.18	0.09	<b>-0.59</b>	-0.17
PA	0.12	<b>1.00</b>	-0.03	0.18	0.12	-0.09	0.05	0.01	0.11	-0.03	-0.36	0.25	0.47	0.41	0.27	-0.30	0.16
VPR	0.17	-0.03	<b>1.00</b>	-0.29	0.45	-0.01	-0.25	-0.21	0.17	-0.16	-0.31	-0.05	-0.25	0.13	0.15	-0.07	0.14
pH	0.39	0.18	-0.29	<b>1.00</b>	0.05	-0.21	-0.26	-0.20	<b>0.60</b>	-0.13	0.05	0.28	-0.22	0.20	-0.22	-0.12	0.17
DO	0.51	0.12	0.45	0.05	<b>1.00</b>	0.15	0.02	0.10	0.25	0.10	-0.12	0.33	<b>-0.52</b>	0.15	0.51	-0.11	0.19
Temp	0.17	-0.09	-0.01	-0.21	0.15	<b>1.00</b>	<b>0.90</b>	<b>0.94</b>	-0.08	<b>0.94</b>	-0.28	0.31	-0.33	-0.02	0.26	-0.32	0.00
Cond	-0.02	0.05	-0.25	-0.26	0.02	<b>0.90</b>	<b>1.00</b>	<b>0.99</b>	-0.27	<b>0.92</b>	-0.11	0.17	-0.06	0.09	0.17	-0.15	0.08
Na <sup>+</sup>	0.08	0.01	-0.21	-0.20	0.10	<b>0.94</b>	<b>0.99</b>	<b>1.00</b>	-0.17	<b>0.96</b>	-0.14	0.26	-0.21	0.04	0.18	-0.20	0.05
Mg <sup>2+</sup>	0.46	0.11	0.17	<b>0.60</b>	0.25	-0.08	-0.27	-0.17	<b>1.00</b>	0.00	-0.45	<b>0.74</b>	-0.33	0.19	-0.06	<b>-0.56</b>	0.21
Cl <sup>-</sup>	0.20	-0.03	-0.16	-0.13	0.10	<b>0.94</b>	<b>0.92</b>	<b>0.96</b>	0.00	<b>1.00</b>	-0.24	0.41	-0.30	-0.09	0.18	-0.29	-0.07
NO <sub>3</sub> <sup>-</sup>	<b>-0.58</b>	-0.36	-0.31	0.05	-0.12	-0.28	-0.11	-0.14	-0.45	-0.24	<b>1.00</b>	-0.49	-0.15	-0.02	-0.22	<b>0.89</b>	0.10
NH <sub>4</sub> <sup>+</sup>	0.38	0.25	-0.05	0.28	0.33	0.31	0.17	0.26	0.74	0.41	-0.49	<b>1.00</b>	-0.31	-0.06	0.37	<b>-0.69</b>	-0.02
HCO <sub>3</sub> <sup>-</sup>	-0.40	0.47	-0.25	-0.22	<b>-0.52</b>	-0.33	-0.06	-0.21	-0.33	-0.30	-0.15	-0.31	<b>1.00</b>	0.20	0.02	0.01	-0.04
<sup>238</sup> U	-0.18	0.41	0.13	0.20	0.15	-0.02	0.09	0.04	0.19	-0.09	-0.02	-0.06	0.20	<b>1.00</b>	-0.16	0.06	<b>0.89</b>
<sup>226</sup> Ra	0.09	0.27	0.15	-0.22	0.51	0.26	0.17	0.18	-0.06	0.18	-0.22	0.37	0.02	-0.16	<b>1.00</b>	-0.16	-0.28
<sup>222</sup> Rn	<b>-0.59</b>	-0.30	-0.07	-0.12	-0.11	-0.32	-0.15	-0.20	-0.56	-0.29	<b>0.89</b>	<b>-0.69</b>	0.01	0.06	-0.16	<b>1.00</b>	0.04
<sup>210</sup> Po	-0.17	0.16	0.14	0.17	0.19	0.00	0.08	0.05	0.21	-0.07	0.10	-0.02	-0.04	<b>0.89</b>	-0.28	0.04	<b>1.00</b>

VA: viral abundances, PA: Prokaryotes abundances, Na: Sodium, Mg: Magnesium, Cl: Chlorides, NO<sub>3</sub>: Nitrates, HCO<sub>3</sub>: Carbonates, Cond: Conductivity, DO: Percentage of dissolved oxygen, Temp: Temperature, DR: Gamma (γ) dose radiation, <sup>222</sup>Rn: <sup>222</sup>Rn activity, <sup>238</sup>U: <sup>238</sup>U activity, <sup>210</sup>Po: <sup>210</sup>Po activity, <sup>226</sup>Ra: <sup>226</sup>Ra activity. Values in bold are significant at p value (alpha=0.05).